INFECTION AND IMMUNITY, Jan. 2004, p. 478–488 Vol. 72, No. 1
0019-9567/04/$08.00+0 DOI: 10.1128/IAI.72.1.478–488.2004

TraJ-Dependent *Escherichia coli* K1 Interactions with Professional Phagocytes Are Important for Early Systemic Dissemination of Infection in the Neonatal Rat

Val T. Hill,[1] Stacy M. Townsend,[1] Robyn S. Arias,[1,2] Jasmine M. Jenabi,[1] Ignacio Gomez-Gonzalez,[1,2] Hiroyuki Shimada,[1,2] and Julie L. Badger[1,2]*

Department of Pathology, Childrens Hospital Los Angeles,[1] and University of Southern California School of Medicine,[2] Los Angeles, California 90027

Received 11 June 2003/Returned for modification 11 August 2003/Accepted 26 September 2003

***Escherichia coli* is a major cause of neonatal bacterial sepsis and meningitis. We recently identified a gene, *traJ*, which contributes to the ability of *E. coli* K1 to penetrate the blood-brain barrier in the neonatal rat. Because very little is known regarding the most critical step in disease progression, translocation to the gut and dissemination to the lymphoid tissues after a natural route of infection, we assessed the ability of a *traJ* mutant to cause systemic disease in the neonatal rat. Our studies determined that the *traJ* mutant is significantly less virulent than the wild type in the neonatal rat due to a decreased ability to disseminate from the mesenteric lymph nodes to the deeper tissues of the liver and spleen and to the blood during the early stages of systemic disease. Histopathologic studies determined that although significantly less or no mutant bacteria were recovered from the spleen and livers of infected neonatal rats, the inflammatory response was considerably greater than that in wild-type-colonized tissues. In vitro studies revealed that macrophages internalize the *traJ* mutant less frequently than they do the wild type and by a morphologically distinct process. Furthermore, we determined that tissue macrophages and dendritic cells within the liver and spleen are the major cellular targets of *E. coli* K1 and that TraJ significantly contributes to the predominantly intracellular nature of *E. coli* K1 within these professional phagocytes exclusively during the early stages of systemic disease. These data indicate that, contrary to earlier indications, *E. coli* K1 resides within professional phagocytes, and this is essential for the efficient progression of systemic disease.**

Although many advances have been made in diagnostics, therapeutics, and supportive care, bacterial sepsis and meningitis continue to be diseases with unacceptable rates of morbidity and mortality. Epidemiological and genotyping studies have shown that *Escherichia coli* is the most common gram-negative bacterium to cause septicemia and meningitis during the neonatal period (26, 39). The mortality rate of neonatal *E. coli* meningitis is between 15 and 40%; furthermore, nearly 50% of meningitis survivors have neurological sequelae (14, 26, 39). Significant neurological complications that occur in neonatal patients with bacterial meningitis include behavioral disorders, hearing loss, delayed development, impaired vision, mental retardation, motor abnormalities, and seizures (26, 40). Although there is great diversity in *E. coli* serotypes (e.g., O antigens, K capsule, and flagellar antigens), it is apparent from epidemiological studies that strains possessing the K1 capsular polysaccharide are the predominant isolates as the etiological agents of *E. coli* neonatal sepsis and meningitis (33, 40).

Neonatal *E. coli* infections are spread both vertically, from mother to infant, and horizontally, from hospital staff or other infected neonates (33). Approximately 50% of childbearing-aged women are colonized with *E. coli* K1, and nearly 77% of all newborns are colonized within the second day of life (33). The estimated annual incidence of *E. coli* neonatal sepsis is approximately between 1 and 4 of 1,000 live births for full-term and premature infants, respectively (14, 35). The primary route of infection is oral contamination, usually due to *E. coli* being transferred from the maternal to the infant gastrointestinal (GI) tract at time of birth. Following intestinal colonization, bacteria translocate through the GI mucosa to extraintestinal sites of mesenteric lymph nodes (MLN), liver, spleen, and the blood. *E. coli* K1 then multiplies systemically within the bloodstream, reaching a necessary threshold of bacteremia, after which bacteria invade the central nervous system.

The exceptional virulence of *E. coli* K1 has been exemplified in several animal models (2, 7, 9, 16, 22, 25, 27, 29, 34). In particular, the neonatal rat as an animal model provides a system that closely parallels the events of neonatal human *E. coli* K1 infections. For example, similar to human infections, infections in the neonatal rat demonstrate age dependency (e.g., 1- to 5-day-old rat pups), a natural route of infection (e.g., oral), gut colonization and translocation, dissemination to deeper tissues, and a level of bacteremia necessary prior to penetration of the blood-brain barrier (BBB) (2, 7, 22, 27, 28, 34).

The ability of *E. coli* K1 to colonize and translocate in the gut, disseminate to deeper tissues, cause bacteremia, and penetrate the BBB involves a complex process of multiple steps of bacterium-host interactions, including attachment, invasion, avoidance, and/or survival of host immune responses. Several bacterial factors have been identified for some of these disease steps. For example, recent work by Martindale et al. deter-

* Corresponding author. Mailing address: Department of Pathology, Childrens Hospital Los Angeles, Keck School of Medicine, University of Southern California, 4650 Sunset Blvd., M.S. #103, Los Angeles, CA 90027. Phone: (323) 669-4625. Fax: (323) 671-1538. E-mail: jbadger@chla.usc.edu.

mined that lipopolysaccharide (LPS) contributes to *E. coli* K1 colonization within the small bowel of the infant rat (25). In addition, some LPS surface antigens play a role in *E. coli* K1 resistance against complement-mediated lysis (22, 28, 38) and systemic infection in the neonatal rat (12, 17, 29, 36). In addition to LPS, type 1 pili contribute to neonatal rat intestinal colonization and spreading within a host population (7, 8, 18, 25). The virulence of *E. coli* K1 has been classically attributed to the antiphagocytic phenotype of this organism. For example, the K1 polysaccharide capsule is critical for bacterial survival in blood and for systemic infection (2, 24, 32) via its properties of being poorly immunogenic (21), interfering with the activation of the alternative complement fixation cascade (26, 32, 37), and inhibiting neutrophil-mediated opsonophagocytosis (10, 28, 37). However, these studies that highlighted *E. coli* K1 antiphagocytic properties had several limitations, including the absence of an examination of the early stages of natural systemic dissemination or the potential importance of macrophages in the disease process.

One of the last steps in the multistep disease process of *E. coli* K1 is meningitis. Outer membrane protein A (OmpA) has been shown to contribute to *E. coli* K1 invasion of the BBB (30) and virulence by way of its ability to confer serum resistance (via alteration of the classical complement pathway) (44). IbeA is a 50-kDa outer membrane protein that mediates specific *E. coli* K1 interactions and the invasion of the BBB (20). Furthermore, the ability of *E. coli* K1 organisms to penetrate the BBB as viable bacteria has been shown to require the K1 capsule (19). Lastly, a BBB invasion gene with significant homology to *traJ* of various F-like plasmid *tra* operons has recently been identified. It has been shown that *traJ* contributes to the ability of *E. coli* K1 to invade the central nervous system and cause meningitis in the neonatal rat (5, 6). In summary, although the first and last steps of neonatal *E. coli* K1 disease (colonization and meningitis, respectively) have been widely investigated, the virulence determinants and/or mechanisms responsible for dissemination to the lymphoid tissues from the GI tract after the natural route of infection have not been identified. For this study, we sought to obtain a better understanding of *E. coli* K1 pathogenesis and to determine whether TraJ plays a role in other stages of *E. coli* K1 neonatal disease.

MATERIALS AND METHODS

Bacterial strains and culture conditions. *E. coli* K1 strain E44 is a spontaneous rifampin-resistant mutant derived from a cerebrospinal fluid (CSF) isolate, RS218 (O18:K1:H7) (44). JLB9(*traJ*) is a stable *traJ* disruption mutant derived from *E. coli* K1 strain E44 (5). For all experiments, bacteria were aerobically grown for 14 h at 37°C in brain heart infusion broth(Difco Laboratories) with rifampin (100 μg ml^{-1}) for E44 and with rifampin (100 μg ml^{-1}) and chloramphenicol (25 μg ml^{-1}) for JLB9(*traJ*). Under various environmental growth conditions, E44 and JLB9(*traJ*) elicit similar growth curves and grow to equivalent culture densities in vitro (data not shown) (5, 6).

Newborn rat model of systemic infection. Sprague-Dawley (Jackson Laboratories) pregnant rats with timed conception (embryonic day 14) were obtained and gave birth in our vivarium (embryonic day 21). Each adult rat and their pups (average litter size, 12) were housed in a solid polypropylene opaque cage under a small-animal isolator (Forma Scientific, Inc.). All experiments began when the pups were 2 to 4 days old. For oral infections of the desired strain, entire litters (~12 pups) were orally infected with saline containing the indicated number of CFU (10-μl total volume) via a P-20 Pipetteman and tip. Neonatal rat pups, by instinct, suck and ingest the entire bacterial suspension. For intraperitoneal (i.p.) inoculations, bacterial saline suspensions containing the indicated number of CFU (100-μl total volume) were injected into the i.p. cavity of the rat pup. At the indicated time points, the rat pups were anesthetized with isoflurane and 10- to 50-μl volumes of blood and CSF samples were collected via intracardiac and cisterna magnum punctures, respectively, as previously described (4). Ten-microliter samples of CSF and blood were inoculated into L broth containing the appropriate antibiotics. In addition, to quantify bacteria in blood, 10-μl samples of blood were also plated on agar plates containing the appropriate antibiotics. Due to the limited availability of sample volumes of neonatal rat CSF, only a qualitative assessment was made for these samples (i.e., 10 μl of CSF sample inoculated directly into L broth). The limit of detection was 50 CFU/ml of fluid obtained. The rats were then euthanized, and liver, spleen, MLN, and descending stool-filled colon samples were aseptically collected in that order. Tissues were weighed and homogenized in phosphate-buffered saline (PBS). The number of bacteria present in tissues was determined by plating serial dilutions on appropriate antibiotic plates. The limit of detection was 50 CFU/g of tissue sample. Mutant bacteria isolated from tissues or blood maintained the genetic mutation as assessed by antibiotic resistance.

For 50% lethal dose (LD_{50}) studies, five groups of six 2-day-old rat pups were infected either via i.p. injection or oral inoculation with 10-fold dilutions of bacterial suspension in PBS (0 to 5,000 CFU and 10^3 to 10^7 CFU for i.p. and oral inoculations, respectively). For oral infections, rat pups were monitored twice a day for 10 days. For i.p. infections, rat pups were monitored every 4 h for 24 h. LD_{50}s were calculated by the method of Reed and Muench (31). The average day of death was calculated from the results of combined experiments including all doses tested. All animal experiments were performed according to protocols approved by the CHLA Institutional Animal Care and Use Committee.

PMN isolation and migration assays. Polymorphonuclear leukocytes (PMNs) were isolated from human peripheral blood. Briefly, peripheral blood from healthy donors was drawn into heparinized syringes. Five percent dextran was added per 10 ml of whole blood collected and gently mixed. Red blood cells were allowed to sediment, and the resultant supernatant was subjected to Ficoll-Hypaque density gradient centrifugation (Nycomed). Residual red blood cells were removed by lysis in cold NH_4Cl buffer. Cells were then subjected to a series of gentle saline washes and resuspended in Hanks balanced salt solution ($HBSS^+$). PMNs with greater than 95% viability and purity, as assessed by trypan blue staining, were used within 1 h of isolation. For PMN migration assays, PMNs were labeled with Calcein AM (Sigma-Aldrich) per the manufacturer's protocol. Calcein AM fluorescent labeling does not inhibit metabolic properties, superoxide production, or chemotaxis of leukocytes (13, 23). Migration assays were performed in transwell plates with 5-μm-pore-size filters (Costar). Approximately 10^6 PMNs were added to upper chambers containing 0.5 ml of $HBSS^+$. The lower chamber contained a 0.5-ml total volume of $HBSS^+$ containing the test strain or *N*-formyl-L-methionyl-L-leucyl-L-phenylalanine (fMLP) (Sigma-Aldrich). We assessed the ability of wild-type and JLB9(*traJ*) strains and the supernatants of respective bacterial cultures to influence PMN migration across the membrane to the lower chamber. Positive migration control included the addition of the chemoattractant fMLP at concentrations of 10^{-5} to 10^{-7} M. Transwell plates were incubated for 45 min at 37°C with 5% CO_2, and PMN migration was enumerated by flow cytometry. Results were calculated as the percentage of added Calcein AM-labeled PMNs that migrated to the bottom chamber.

Bacterial interactions with phagocytes. Gentamicin protection assays (i.e., invasion assays) were performed as described previously (5, 6). For phagocytosis and intracellular survival assays, essentially the same protocol was used, except that 10^5 bacteria were added to macrophages or PMNs (multiplicity of infection, 15). U937 human macrophages (ATCC CRL-1593.2) were activated by pretreatment with 0.1 μg of phorbol 12-myristate 13-acetate (PMA) (Sigma-Aldrich) per ml for 24 h. Bacteria and phagocytes were incubated for 45 min, and subsequent gentamicin treatments were done for 45 min. To determine the effects of preopsonizing the bacteria in the macrophage uptake and survival assays, the bacteria were first mixed with experimental media containing 2.5% human pooled serum (Omega Inc.) and then added to macrophage monolayers as described above. To evaluate long-term survival within the macrophages, extended incubations were performed with a lower level of gentamicin (20 μg/ml). Percent survival was calculated as the number of recovered CFU divided by the number of CFU initially intracellular multiplied by 100. The ability of strains to associate (i.e., bind or attach) with eukaryotic cells was evaluated postincubation at 37 and 4°C for 15 min. Cells were extensively washed and lysed with 0.5% Triton-X, and recoverable CFU was determined. Assays were performed in triplicate and repeated at least three times.

Rat peritoneal macrophages were isolated by i.p. injection of a mixture containing 40 ml of RPMI 1640, 5% fetal bovine serum, and 5 U of heparin per ml into euthanized adult rats. Following i.p. injection, the rats were massaged to dislodge peritoneal cells, and lavage fluids were removed. Peritoneal cells were

TABLE 1. Summary of low-dose oral infection in neonatal rats[a]

E. coli K1 strain	Rat pup no.	Viable count of bacteria in:			
		Colon (CFU/g)	Liver (CFU/g)	Spleen (CFU/g)	Blood (CFU/ml)
E44 (wild type)	1	1.4×10^7	8.5×10^7	3.0×10^8	3.0×10^4
	2	3.0×10^7	6.3×10^6	2.5×10^5	1.5×10^4
	3	2.6×10^7	1.7×10^5	2.5×10^5	1.5×10^4
	4	1.0×10^4	1.2×10^3	5.0×10^3	4.0×10^2
JLB9(*traJ*)	1	1.1×10^7	0	0	0
	2	2.0×10^4	2.5×10^3	5.0×10^3	0
	3	9.0×10^6	0	0	0
	4	1.2×10^9	3.3×10^3	0	0
	5	4.0×10^6	0	0	0
	6	1.9×10^7	0	2.5×10^3	0

[a] Oral doses of 10^4 bacteria were given to neonatal rat pups [E44, $n = 4$; JLB9(*traJ*), $n = 6$]. Indicated tissues were collected from infected animals day 3 postinoculation, and viable counts were determined. Data are presented as CFU per gram of tissue or per milliliter of blood. Data presented are representative of several experiments with similar results.

centrifuged, resuspended in media, and plated. Cells were allowed to attach, gently washed to remove nonadherent cells, incubated, and used ~24 h later. Phagocytosis assays were performed as described above.

Histopathology. In parallel to the oral infection kinetic experiments, tissues of infected animals were examined for inflammation. Sections of spleens and livers were harvested and fixed in 4% buffered formalin. Fixed tissues were embedded in paraffin blocks, sectioned at 4- to 5-μm thicknesses, mounted onto glass slides, and stained with hematoxylin and eosin. Histopathological analysis was performed in a blinded fashion by a pathologist (I.G.-G.). The nature and degree of inflammation were graded with an arbitrary scale: 0, no inflammation; +, focal (not clustered) neutrophils; ++, frequent but sparse neutrophils; +++, clustering of neutrophils; ++++, dense clustering of neutrophils. Tissues collected from PBS-infected animals were analyzed in parallel as controls.

Immunofluorescence microscopy. The association rate of *E. coli* K1 and specific phagocytes during early dissemination was determined as follows. Four-day-old neonatal rats were orally infected with 10^7 wild-type *E. coli* K1 strain E44 or *traJ* mutant JLB9 bacteria. On days 1 and 3 post-oral inoculation, livers and spleens were removed. One half of each organ was homogenized and plated for CFU, and the numbers of CFU per gram of tissue were determined (level of detection, 50 CFU/g). The remaining tissue samples were mounted in Tissue Tek-OCT and snap-frozen in 2-methyl butane. Ten-micrometer sections were subjected to immunofluorescent microscopy with the following antibodies: anti-*E. coli* K1 (Abcam, Inc.), anti-ED-2 (Research Diagnostics, Inc.), anti-Ox-62 (Research Diagnostics, Inc.), anti-ED-1 (Research Diagnostics, Inc.), anti-mouse immunoglobulin G-fluorescein isothiocyanate (IgG-FITC) (Sigma-Aldrich), anti-mouse IgG-Cy3 (Sigma-Aldrich), and anti-mouse IgG-Cy5.5 (Rockland, Inc.). To ensure complete saturation or to prevent cross-staining, all incubations were performed with dilutions of 1:100 in 15% normal goat serum (Sigma-Aldrich) in 1× PBS (G-PBS). Unless specified, incubations were done for 1 h at room temperature in the dark. Following all incubations, extensive washes were performed with 1× PBS. Briefly, frozen sections were rehydrated in PBS and subsequently blocked with G-PBS for 30 min. Phagocyte-specific primary antibody was applied and detected with anti-mouse IgG-FITC. Sections were then permeabilized with 0.5% Triton-X–G-PBS for 15 min. *E. coli* K1 was detected via the addition of a primary antibody with subsequent incubation with anti-mouse IgG-Cy3. Sections were then mounted and coverslips were applied by using Vectashield mounting medium containing the nuclear stain 4′,6′-diamidino-2-phenylindole (DAPI) (Vector Laboratories) and allowed to air dry. Sections were viewed with a ×63 oil objective on a Leica DM-RXA fluorescence microscope. Images were taken by using excitation and emission filters as appropriate for the fluorochromes employed. Image analysis was performed with EasyFish (Applied Spectral Imaging, Inc.). The experiments performed indicated that the anti-*E. coli* K1 antibody equally stains viable and nonviable organisms. As a control, the above experiments were performed with the primary antibodies omitted and yielded negative secondary staining. Furthermore, complete saturation of primary and secondary antibodies was confirmed by a lack of overlapping staining (i.e., FITC and Cy3 overlays were viewed as yellow). Entire tissue sections from the livers and spleens of multiple animals (i.e., $n = 4$ to 6) were examined, and positive staining was quantified. Bacteria were considered to be associated when stained bacteria were in very close or immediate proximity to stained nuclear material (with DAPI) of FITC positively stained phagocytes. Results are presented by the following formula: association rate = [(total number of bacteria) × (percent associated with stained cell type)]/total number of stained cells. From three independent experiments, the data for entire tissue sections (containing 500 to 1,000 positively stained phagocytes and 0 to 500 stained *E. coli* K1 bacteria) were averaged and presented as means ± standard errors of the means (SEM).

The percentage of total bacteria that was contained within specific professional phagocytes was determined as described above, except that a step-wise permeabilization staining procedure, which determines intracellular versus extracellular bacteria, was used. Sections were stained as described above, except that the extracellular bacteria were detected before permeabilization by utilizing secondary antibody conjugated to fluorochrome Cy3. The sections were then permeabilized as described above, and intracellular bacteria were stained with a differing secondary antibody conjugated to Cy5.5. To capture and characterize the infrared fluorescence-emitting Cy5.5 stain, the Cy5.5 signal was pseudocolored with either aqua or fuchsia. Thus, intracellular bacteria were identified by a fuchsia or aqua color, whereas extracellular bacteria were identified by a red color. No overlay of Cy3 and Cy5.5 was detected, confirming complete saturation of staining. Furthermore, stained sections were examined with a Leica SP1 confocal microscope to substantiate the intracellular nature of bacteria and confirm staining patterns viewed in *xy*, *xz*, and *yz* orthogonal projections. Results are presented by the following formula: percent intracellular bacteria = [number of stained intracellular bacteria (i.e., $Cy5.5^+$)/total bacteria associated with positive stained cell (i.e., Cy5.5 plus Cy3)] × 100. From several experiments, the data for entire tissue sections (containing 500 to 1,000 positively stained phagocytes and 0 to 500 stained *E. coli* K1 bacteria) were averaged and presented as means ± SEM.

Electron microscopy. Transmission electron microscopy (TEM) was performed on PMA-stimulated U937 macrophages incubated with *E. coli* K1 as described above. After 30 min of incubation, the macrophage monolayer was washed four times with RPMI 1640 and gently scraped from the plastic surface. The cell slurry was then centrifuged for 10 min at 7,000 × *g*. The cell pellet was resuspended and fixed with 2.5% glutaraldehyde in 0.1 M PBS. Cells were washed and postfixed with 2% OsO_4 for 1 h, rinsed, dehydrated through graded ethanol solutions, and embedded in polypropylene oxide. Ultrathin sections were cut, mounted on collodion one-hole grids, stained with uranyl acetate and lead citrate, and examined by TEM with a Phillips CM transmission electron microscope.

Statistical analysis. Differences in tissue colonization among groups of rats post-oral infection were analyzed as follows. To stabilize any potential variances, a transformation, $\ln(x + 0.5)$, was applied to each data point (day 1 postinfection data consist of data from a total of five independent experiments, where the number of rats (n) was 30 for each strain tested, and data from day 5 consist of data from two independent experiments, where n was 11 for each strain tested). Repeated-measure analysis of variance was performed by using NCSS 2000 software (Statistical Solutions, Inc.). Descriptive reports were run by experiment and strain to compute mean and statistical deviations. Differences between strains with respect to macrophage uptake data were analyzed by Student's t test. Each experiment was repeated at least three times. A P value of ≤ 0.05 was considered significant.

RESULTS

TraJ contributes to *E. coli* K1 virulence in the neonatal rat. LD_{50} analysis was performed with the wild type (E44) and the *traJ* mutant (JLB9) in neonatal rats post-oral and -i.p. inoculation. Five groups of six 2-day-old rat pups were infected with 10-fold-increasing doses of 10^3 to 10^7 CFU administered orally or 0 to 6×10^3 CFU administered i.p. of either wild-type E44 or JLB9(*traJ*), and LD_{50} values were calculated by the Reed-Muench formula (32). By using death as an end point, the virulence of the wild-type strain was 56-fold higher after oral challenge (LD_{50}, 2.5×10^4) than that of JLB9(*traJ*) (LD_{50}, 1.4×10^6). Interestingly, there was a difference in the average day of death for animals infected with the wild type and those infected with JLB9(*traJ*) (5.7 and 6.9 days, respectively). The LD_{50}s post-i.p. challenge, a route of infection that bypasses gut colonization and translocation to the MLN, determined that the virulence of the *traJ* mutant is 15-fold lower than that of the wild type when administered i.p. [LD_{50} of the wild type, 2.5×10^2; LD_{50} of JLB9(*traJ*) mutant, 3.7×10^3].

JLB9(*traJ*) is attenuated in dissemination to the liver and spleen post-oral infection. To determine the precise steps in which a *traJ* mutation affects *E. coli* K1 virulence, we examined the kinetics of infection. Neonatal rat pups were orally infected with either wild-type E44 or JLB9(*traJ*). MLN, liver, spleen, and blood samples were collected 1, 3, and 5 days postinoculation, and recoverable CFU were determined. For our initial experiments, we assessed a low dose of 1.0×10^4 bacteria. We found that on day 3 post-oral inoculation of 1.0×10^4 bacteria, the wild type and JLB9(*traJ*) showed comparable levels of neonatal rat gut colonization (Table 1). In contrast, the *traJ* mutant was attenuated in its ability to colonize the deeper tissues (liver and spleen) and blood (Table 1). Subsequent experiments performed with a higher dose of 5×10^7 CFU substantiated that the *traJ* mutant and wild-type E44 were equally capable of colonizing the GI tract (data not shown) and translocating from the gut to the MLN (Fig. 1A). Furthermore, similar to the lower-dose experiments, the *traJ* mutant demonstrated a loss of or significantly lower levels of recoverable bacteria from the liver, spleen, and blood 24 h post-oral inoculation with 5×10^7 CFU (Fig. 1A). By day 5 postinoculation, although we observed some animal-to-animal variation in bacterial loads within tissues and blood, it was clear that JLB9(*traJ*) colonization levels were able to "catch up" to wild-type colonization levels in all tissues and blood by day 5 post-oral inoculation with 5×10^7 CFU (Fig. 1B).

Neonatal rats were next inoculated with 250 CFU (1 LD_{50}) by i.p., a route that bypasses the GI tract. We found no difference between the abilities of the mutant and the wild-type strain to colonize the liver, spleen, or blood 6 h postinoculation (Fig. 2A). These data indicate that when bacteria are administered systemically, the wild type and JLB9(*traJ*) are equally capable of targeting and colonizing the liver and spleen. At 24 h postinoculation, 8 of 10 (80%) of animals infected with the wild type were dead, whereas 1 of 9 (11%) JLB9(*traJ*)-infected animals died (Fig. 2B). At the 24-h time point, there was again no appreciable difference in bacterial loads within the liver, spleen, or blood for the remaining viable animals i.p. infected with the wild type or JLB9(*traJ*) (Fig. 2B). These results remained unchanged when data collected from tissues

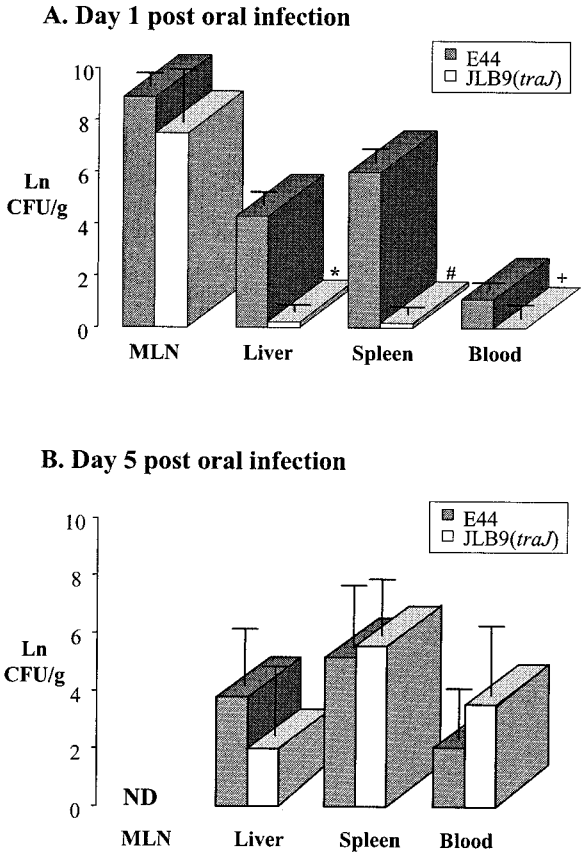

FIG. 1. Kinetics of *E. coli* K1 infection after an oral dose of 5×10^7 bacteria. Bacteria (5.0×10^7 CFU) were given in oral doses to neonatal rat pups. Days 1 (A) and 5 (B) postinoculation, the indicated tissues were collected from wild-type (E44)- or *traJ* mutant (JLB9)-infected animals, and viable counts were determined. The numbers of CFU per gram of tissue or per milliliter of blood were calculated, and values were transformed [$\ln(x + 0.5)$]. Data are presented as the mean ± standard deviation of results from five independent experiments ($n = 30$ pups per strain) (A) and two independent experiments ($n = 11$ pups per strain) (B). *, $P = 0.005$; #, $P < 0.0001$; +, $P = 0.04$. A P value of ≤ 0.05 was considered statistically significant. ND, not determined.

of dead animals were also included in the data sets. Of interest, the frequency with which i.p. JLB9(*traJ*)-infected animals developed meningitis, as assessed by positive CSF cultures, was 50% lower than that of animals infected with wild-type E44 (100%) (Fig. 3B). These results are in accordance with previous observations that the *traJ* mutant is less able to penetrate the BBB in vitro and in vivo after systemic infection (6).

JLB9(*traJ*) elicits an altered inflammatory response in the liver and spleen post-oral infection. To examine the potential role of the host inflammatory response in JLB9(*traJ*)'s inability to efficiently colonize the liver and spleen at day 1 post-oral inoculation, we performed a histopathological analysis on these tissues. For this purpose, histological sections of livers and spleens from neonatal rat pups orally infected with 5×10^7 bacteria were analyzed day 1 post-oral inoculation in parallel with the oral infection kinetics studies presented in Fig. 1A. We found that although there were significantly less or no recoverable bacteria from the livers and spleens of the

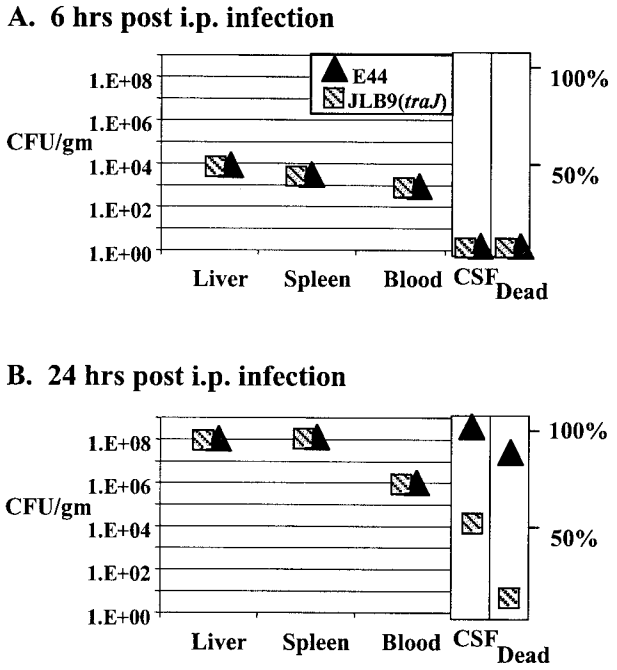

FIG. 2. Kinetics of *E. coli* K1 infection at 6 and 24 h after i.p. inoculation. Neonatal rats were i.p. infected with 2.5×10^2 bacteria. Recoverable numbers of CFU were determined for tissues, and fluids were harvested from viable animals at the indicated time points; data for animal groups were averaged and are presented graphically. Data for tissue and blood are presented as CFU per gram of tissue or per milliliter of blood, respectively. Data for CSF culture-positive samples are presented as a percentage of the population sampled that were culture positive. Results remained the same when tissues harvested from dead animals were included in the data sets. The percentage of dead animals were collected for all infected animals (6 h, $n = 4$ per strain; 24 h for E44, $n = 10$; and 24 h for JLB9[*traJ*], $n = 9$).

TABLE 2. Tissue inflammation compared to recoverable CFU day 1 post oral infection[a]

Strain	Rat pup no.	Inflammatory score in:		
		Spleen	Liver	
			Lobule	Portal tract
E44 (wild type)	1[b]	0	0	0
	2	0	+	+
	3[b]	+	+	++
	4[b]	0	+	++
	5[b]	0	++	++
	6	0	+	++
JLB9(*traJ*)	1	++	++	++++
	2	++	++	+++
	3	+	+	+++
	4	+	+	++
	5	+	+	++
	6	+	++	+++

[a] Neonatal rats were orally infected with 5.0×10^7 bacteria (E44, $n = 6$; JLB9(*traJ*), $n = 6$). On day 1 postinoculation, tissues were harvested and processed for recoverable CFU and histological examination as described in Materials and Methods. Tissue sections were examined in a blinded fashion and arbitrarily quantified. Scale: 0, no inflammation; +, focal (not clustered) neutrophils; ++, frequent but sparse neutrophils; +++, clustering of neutrophils; ++++, dense clustering of neutrophils. The results are presented as a representative experiment of several performed with similar results.

[b] Recoverable CFU is present in the spleen and/or liver of that infected animal.

JLB9(*traJ*)-infected animals than from the wild-type-infected animals, there was considerably more of an inflammatory response, as indicated by infiltrating neutrophils (Table 2). The increase in neutrophils was observed for both tissue types infected with JLB9(*traJ*); however, the increase in inflammation was more pronounced in the portal tracts from the livers of animals infected with the *traJ* mutant (Table 2). Similar results showing profound inflammatory responses in the livers and spleens of the mutant-infected animals compared to those of the wild type, and yet no recoverable mutant bacteria, were obtained on days 5 and 7 post-oral inoculation with the lower dose of 10^4 CFU (data not shown). Of interest, histological analysis of livers and spleens isolated 24 h after i.p. inoculation revealed that there were few or no infiltrating neutrophils in tissues infected by either of the two strains (data not shown). These data suggest that the decrease in virulence of the *traJ* mutant compared to that of the wild type is due to, in part, the ability of the host to recognize, mount an inflammatory response against, and/or effectively kill the infecting mutant bacteria during the oral infection process.

***E. coli* K1 elicits PMN migration in vitro.** Because our data indicated that the *traJ* mutant elicited a profound increase in neutrophil infiltration in the liver and spleen post-oral infection, whereas wild-type *E. coli* K1 did not, we examined the

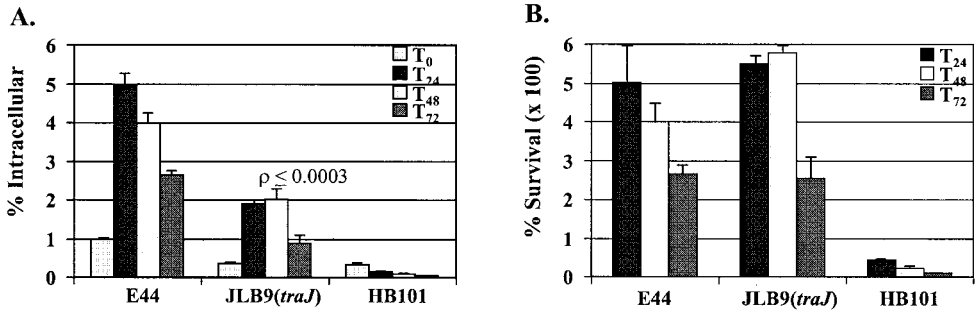

FIG. 3. Ability of *E. coli* K1 to interact with human macrophages. (A) Results are presented as a percentage of inoculum that was intracellular at indicated time points (e.g., $T_{12} = 12$ h). (B) Results are presented as a percentage of T_0 intracellular bacteria surviving over time. Nonpathogenic *E. coli* K-12 strain HB101 was used as a negative control. Data presented are for an experiment performed in triplicate and are representative of several experiments with similar results. All values are the means ± standard deviations.

abilities of the two strains to promote neutrophil migration. For this purpose, we performed PMN migration assays in vitro by using transwell plates with 5-μm-pore-size filters. We found that freshly isolated human PMNs showed a 4.7% ± 1.5% "background" migration (experimental medium alone in bottom chamber), whereas the PMN migration was 40.9% ± 0.2% with the addition of 10^{-7} M fMLP (chemoattractant) to the bottom chamber. Experiments performed with wild-type E44 and JLB9(*traJ*) inoculated in the bottom chamber indicated that the two strains were very comparable in their abilities to induce PMN migration across the transwell filters (i.e., 64.7% ± 5.3% and 68.5% ± 13.0%, respectively). Similar results were seen when culture supernatants of the two respective strains were tested (data not shown).

JLB9(*traJ*) shows decreased internalization by macrophages in vitro. Professional phagocytes, including PMNs and macrophages, are known to be "safe sites" for some pathogenic bacteria. These intracellular sites provide a niche for bacteria to hide from the host defenses and may provide a mechanism for altering host response. We sought to determine whether the interaction of bacteria with macrophages and PMNs was altered for the *traJ* mutant compared to that of the wild type. For this purpose, we assessed the abilities of the two strains to associate, be taken up, and survive within human PMNs and macrophages. Phagocytosis assays performed with PMA-stimulated human macrophage U937 cells showed that JLB9(*traJ*) was internalized at a lower frequency than was wild-type E44 (Fig. 3A). Interestingly, once the bacteria were within the macrophages, the *traJ* mutation had no significant effect on *E. coli* K1 survival (Fig. 3B). In addition, the difference in the abilities of the wild type and mutant to bind or associate was indistinguishable. After 15 min of incubation at 37°C, 1.5% ± 0.00% and 1.1% ± 0.14% of the wild-type and JLB9(*traJ*) inocula, respectively, were associated with macrophages. Similarly, after 15 min of incubation at 4°C, 1.1% ± 0.01% and 0.81% ± 0.01% of the wild-type and JLB9(*traJ*) inocula, respectively, were associated with macrophages. Similar results were observed when bacteria were preopsonized with 2.5% pooled human serum (data not shown). In addition, when experiments were performed with freshly isolated peritoneal macrophages from adult rats, JLB9(*traJ*) maintained its phenotype of decreased internalization compared to that of wild-type *E. coli* K1 (i.e., 0.19% ± 0.01% and 1.59% ± 0.34% intracellular bacteria, respectively). In contrast, phagocytosis assays performed with freshly isolated human PMNs showed no difference in the abilities of the wild type and the *traJ* mutant to associate, be taken up, or survive within human PMNs (data not shown). Furthermore, we found no difference in the abilities of the two strains to invade human epithelial cell lines HEP-2 (tracheal) and HepG-2 (liver) (data not shown). To rule out the possibility that cytotoxic effects of *E. coli* K1 could affect the ability of macrophages to internalize the bacteria, the viability of the eukaryotic cells was assessed by using both trypan blue exclusion and Calcein AM staining. Before infection, the viability of the phagocytes was greater than 95%. There was no significant change in macrophage viability observed during the infection period with either of the two strains tested (data not shown). These results suggest that the *traJ* mutation affects the ability of macrophages to efficiently internalize *E. coli* K1.

Microscopic analysis of *E. coli* K1 and macrophages. Our results from gentamicin protection assays indicate that macrophages take up JLB9(*traJ*) at a lower frequency than that of the wild type; however, because these assays rely on viable bacterial counts, these assays cannot differentiate between uptake efficiency and mechanisms of uptake and/or the nature of bacterial cell-eukaryotic cell interactions. For this purpose, we analyzed the bacteria and eukaryotic cell interactions at the single-cell level via electron microscopy during in vitro macrophage uptake assays. Thus, infected U937 macrophage monolayers were fixed 30 min after incubation with the bacteria and processed for TEM examination. Figure 4A and B shows entry events for *E. coli* K1 after 30 min of incubation with macrophages. For both the wild type and the *traJ* mutant, similar intimate interactions between the bacteria and the cell surface were observed, with some visible condensation of electron-dense particles accumulating within the vicinity of contact. In contrast, the intracellular characteristics of the two strains taken up within macrophages appeared to be different. For example, wild-type *E. coli* K1 strain E44 consistently appeared to be in spacious phagosomes (Fig. 4C), whereas not only was the frequency of observing intracellular JLB9(*traJ*) much lower, but the *traJ* mutant bacteria were always observed to be within tight single-membrane vacuole-like structures (Fig. 4D). Taken together, these data suggest that the mechanisms by which macrophages take up *E. coli* K1 wild-type and *traJ* mutant bacteria differ in both function and efficiency.

***E. coli* K1 associates specifically with professional phagocytes during early dissemination.** Our data thus far suggest that TraJ contributes to efficient *E. coli* K1 dissemination and colonization of the liver and spleen via bacterial interactions with macrophages. Therefore, we next sought to determine if, during early dissemination in the neonatal rat, *E. coli* K1 bacteria were interacting with professional phagocytes, and if so, what were the specific cell types of mononuclear phagocytes. For this purpose, 1 day after oral inoculation of 10^7 bacteria, liver and spleen tissues were collected, the numbers of CFU per gram of tissue were determined, and tissue sections were subjected to immunohistochemical analysis by using monoclonal antibodies against specific markers present on monocytes (ED1), resident tissue macrophages (ED1 and ED2), and dendritic cells (ED1 and Ox-62) and for the presence of *E. coli* K1 bacteria. Similar to earlier results (Fig. 1A), we found that wild-type *E. coli* K1 colonized the liver and spleen at significant levels (i.e., 10^3 to 10^4 CFU/g), whereas the *traJ* mutant showed little or no recoverable bacteria 1 day post-oral infection (i.e., 0 to 60 CFU/g). Immunohistological analysis showed that in the liver, wild-type *E. coli* K1 bacteria were predominately associated with $ED2^+$ cells (i.e., resident macrophages) and, to a lesser extent, dendritic cells ($Ox\text{-}62^+$) (Fig. 5). However, in the spleen, wild-type *E. coli* K1 bacteria were equally associated with dendritic cells ($Ox\text{-}62^+$) and tissue macrophages ($ED2^+$) (Fig. 5). Consistent with these results, in both tissues, wild-type *E. coli* K1 strongly associated with cells that stained positively for ED1, which includes monocytes, macrophages, and dendritic cells (data not shown). Interestingly, liver and spleen samples harvested from animals infected with the *traJ* mutant showed no recoverable bacteria; yet, by utilizing the *E. coli* K1-specific antibody, immunofluorescence microscopy revealed low levels of bacteria in these tissues (i.e., 2- to 10-fold

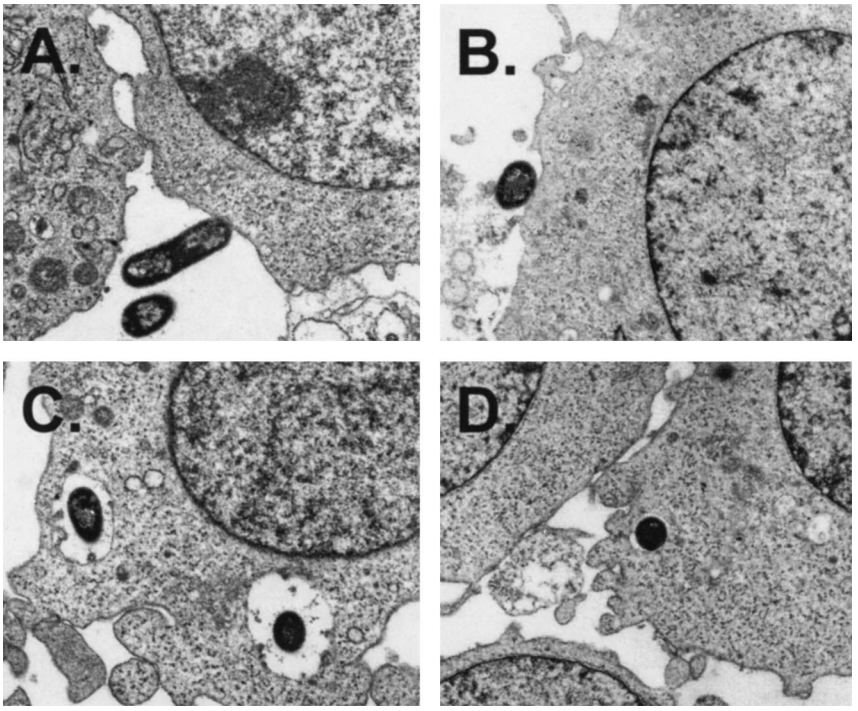

FIG. 4. TEM of *E. coli* K1 interactions with macrophages. TEM demonstrating wild-type (A and C) and *traJ* mutant (B and D) *E. coli* K1 interactions with macrophages at a magnification of ×14,000. (A and B) Extracellular *E. coli* K1 binding or associating with macrophages (wild-type E44 [A] and *traJ* mutant JLB9 [B]) is shown. (C and D) Intracellular *E. coli* K1 was found within membrane-bound vacuole-like structures. Wild-type E44 in spacious phagosomes (C) and JLB9(*traJ*) in smaller and tight vacuoles (D) are shown.

decrease in detectable bacteria compared to that of the wild type). Furthermore, immunohistological analysis indicated that in *traJ* mutant-infected animals, there was no specific cell type associating with the *traJ* mutant in the livers and spleens. Interestingly, although animals orally infected with the wild type showed consistent colonization in the liver and spleen over time (i.e., to day 5) (Fig. 1B), we found that by day 3 post-oral inoculation, the association rate of specific professional phagocytes within the tissues had diminished (Fig. 5). These data indicate that the TraJ-dependent interactions of *E. coli* K1 with particular phagocytes is specific to the early stages of the disease process.

***E. coli* K1 bacteria predominantly reside within specific professional phagocytes during early dissemination and are dependent on TraJ.** Because the *traJ* mutant bacteria are taken up less by macrophages and by a morphologically distinct process in vitro, and because we observed a strong association of *E. coli* K1 with specific phagocytes during early dissemination, we next sought to determine the percentage of *E. coli* K1 bacteria that occur within the specific professional phagocytes (i.e., resident macrophages and/or dendritic cells) during early dissemination in the neonatal rat. For this purpose, tissues were collected day 1 post-oral inoculation of 10^7 bacteria, and the immunohistology staining experiments described above were performed; however, to detect intracellular versus extracellular bacteria associated with the cell types, we performed additional step-wise permeabilization incubations using *E. coli* K1-specific antibodies and secondary antibodies conjugated with differing fluorochromes (i.e., Cy3 and Cy5.5) (Fig. 6A and B). We found that 96.5% ± 3.1% and 68.0% ± 6.4% of wild-type bacteria examined within the spleen and liver, respectively, occurred within $ED2^+$ cells. In contrast, for animals infected with the *traJ* mutant, these tissues showed no recoverable bacteria; of those bacteria observed, only 23.0% ± 2.1% and 30.9% ± 8.4% occurred within $ED2^+$ cells (tissue macrophages) in the spleen and liver, respectively (Table 3). Examinations with the dendritic-cell-specific marker (Ox-62) revealed that again there was a strong association of wild-type bacteria with this specific cell type within the spleen and, to a lesser extent, the liver. For example, 84.8% ± 7.7% and 35.0% ± 5.0% of wild-type bacteria occurred within dendritic cells of the spleen and liver, respectively. In contrast, only 12.0% ± 6.4% and 6.0% ± 2.0% of the observed *traJ* mutant bacteria resided within $Ox\text{-}62^+$ dendritic cells of the spleen and liver, respectively (Table 3). Similar results highlighting the increased frequency of intracellular wild-type *E. coli* K1 bacteria relative to that of the *traJ* mutant bacteria were obtained when these experiments were performed with human U937 macrophages in vitro (data not shown). Furthermore, confocal microscopy substantiated the intracellular relationship among *E. coli* K1 bacteria and specific phagocyte populations during early systemic dissemination in the neonatal rat (Fig. 6C).

DISCUSSION

In previous work, *finP-traJ* was identified as a BBB invasion locus by using two independent experimental approaches (differential fluorescence induction and signature-tagged mutagenesis) (5, 6). *finP-traJ* is homologous to the F-like plasmid conjugation systems. In the F-like plasmid conjugation sys-

tems, *finP* is an antisense transcript that is encoded divergently within the 5′ coding region of *traJ*. TraJ is a positive regulator required for the expression of several structural and regulatory genes necessary for DNA conjugation (15). The expression of *traJ* has been shown to be negatively regulated by FinP via the antisense RNA molecule binding and occluding the ribosome-binding site of the *traJ* transcript (42). Our *E. coli* K1 *traJ* mutant, JLB9(*traJ*), is a result of targeted disruption in the 5′ end of *traJ* (5); therefore, *finP* expression is also altered. It has previously been shown that wild-type *finP-traJ* supplied in *trans* complements the JLB9(*traJ*) mutant invasion phenotype (5, 6). Furthermore, we have determined that several regenerated *traJ* mutants and wild-type *E. coli* K1 strains that overexpress *finP* (which encodes the antisense negative regulator of *traJ*) both show similar mutant phenotypes as JLB9(*traJ*) in vitro and in vivo (unpublished data).

This study was undertaken in efforts to better understand *E. coli* K1 pathogenesis and to potentially elucidate TraJ's role in neonatal disease. We found that after oral challenge, a natural route of infection, the *traJ* mutant was significantly less virulent than the wild type in the neonatal rat, whereas there was a modest (i.e., 15-fold) decrease in virulence for the *traJ* mutant after i.p. inoculation, a route of infection that bypasses gut colonization and translocation to the MLN. Oral-infection kinetics experiments determined that TraJ influences the earlier stages of *E. coli* K1 dissemination from the MLN to the liver and spleen. In contrast, the *traJ* mutation does not affect gut colonization or significantly affect systemic infection after i.p. challenge. To our knowledge, this is the first study examining systemic dissemination of *E. coli* K1 after the natural route of infection in the neonatal rat and particularly one in which a virulence determinant has been identified for this critical step of the disease process.

It was interesting that although the *traJ* mutant was less virulent than the wild type post-oral inoculation and that TraJ's influence on *E. coli* K1 oral infection was predominant in the early dissemination phase of the disease (i.e., day 1 post-oral inoculation), several days later, the *traJ* mutant was able to catch up to the wild-type levels of recoverable bacteria from the liver, spleen, and blood. Histopathological analyses performed in parallel with the oral-infection kinetics experiments revealed that although there was no or significantly less recoverable bacteria in the livers and spleens of animals infected with the *traJ* mutant, these tissues demonstrated substantially more infiltrating neutrophils than the wild-type-infected tissues which contained high levels of recoverable bacteria. Furthermore, immunofluorescence experiments revealed that although no bacteria were recovered from these tissues, there were detectable *traJ* mutant bacteria. We presume that the majority of these *traJ* mutant bacteria are nonviable because in wild-type-infected animals, liver and spleen samples yielded 10^3 to 10^4 CFU/g of tissue (level of detection, 50 CFU/g), yet when examined by immunofluorescence microscopy, the levels of organisms detected by anti-*E. coli*-specific antibody in mutant-infected animals was only approximately 2- to 10-fold lower than that in the wild-type-infected tissues. However, because the *traJ* mutant is able to catch up to the wild-type levels of colonization, there must be a percentage of this mutant population that is viable yet still remains below the levels of detection (CFU per gram of tissue). We found that TraJ

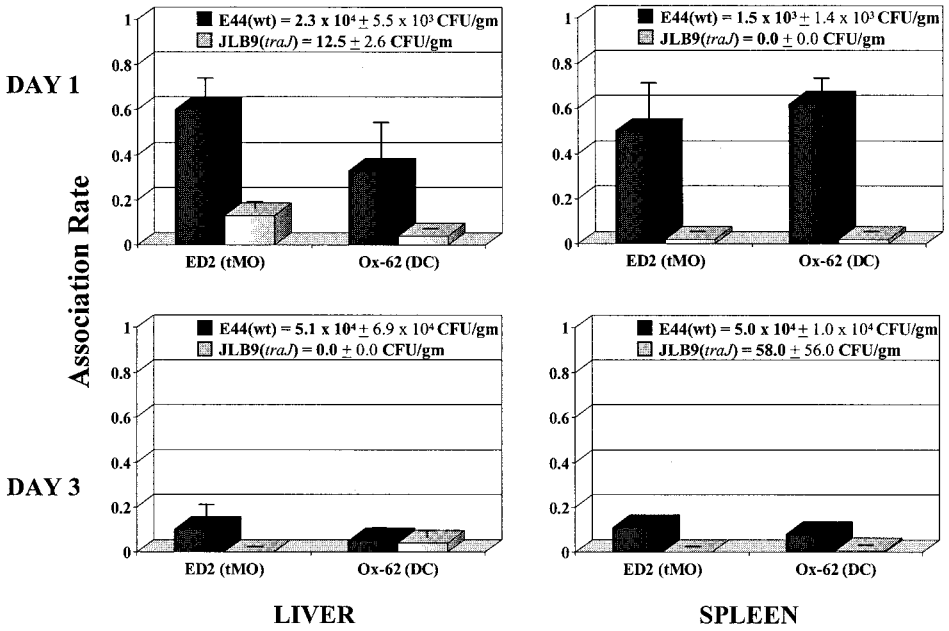

FIG. 5. Association rate of *E. coli* K1 and specific phagocytes during early dissemination. Neonatal rats were orally infected with 5.0×10^7 wild-type *E. coli* K1 or *traJ* mutant JLB9 bacteria. On days 1 and 3 post-oral inoculation, livers and spleens were removed. One half of the organ was homogenized and plated for CFU, and numbers of CFU per gram of tissue were determined. The remaining tissue sample was subjected to immunofluorescence microscopy as described in Materials and Methods. Results are presented by the following formula: association rate = (total number of bacteria × percentage of bacteria associated with stained cell type)/total number of stained cells. Data from three independent experiments were averaged and are presented as the mean ± SEM. DC, dendritic cell; tMO, tissue macrophage; wt, wild type.

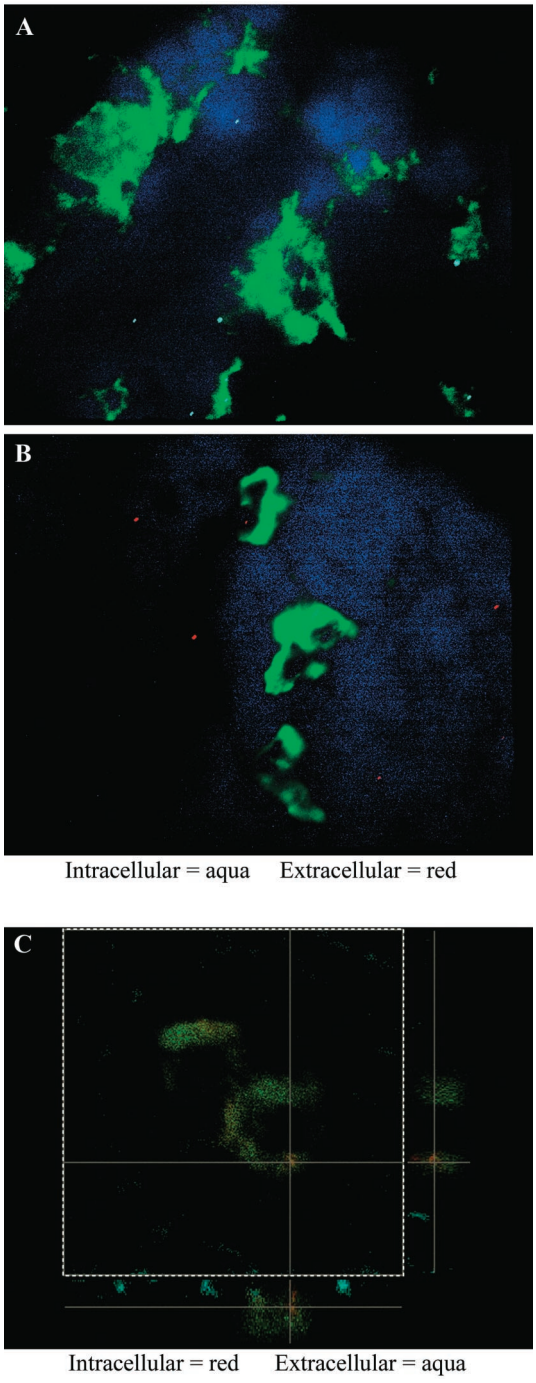

FIG. 6. *E. coli* K1 associates with professional phagocytes during early dissemination. Representative immunohistology analysis of neonatal rat spleens 1 day post-oral infection with *E. coli* K1 is shown. Tissue samples were subjected to immunofluorescent staining for dendritic cell marker Ox-62 and the *E. coli* K1 wild type (A and C) and the *traJ* mutant (B) via step-wise permeabilization as described in Materials and Methods. (A and B) Intracellular bacteria were stained with Cy5.5 (aqua), and extracellular bacteria were stained with Cy3 (red). Tissue sections were also stained with dendritic-cell-specific cell marker Ox-62 (green) and the cell nuclear material stain DAPI (blue). Stained sections were then examined, and images were captured with a Leica DM-RXA fluorescence microscope. (C) Intracellular bacteria were stained with Cy3 (red), and extracellular bacteria were stained with Cy5.5 (aqua). Stained sections were then examined with a Leica SP1 confocal microscope, and images were displayed as *xy*, *xz*, and *yz* orthogonal projections.

TABLE 3. Percentage of associated bacteria within specific professional phagocytes[a]

E. coli K1 strain	% Intracellular bacteria			
	Liver		Spleen	
	ED2 (tMO)	Ox-62 (DC)	ED2 (tMO)	Ox-62 (DC)
E44 (wild type)	68.0 ± 6.4	35.0 ± 5.0	96.5 ± 3.5	84.8 ± 7.7
JLB9(*traJ*)	30.9 ± 8.4[b]	6.0 ± 2.0[c]	23.0 ± 7.1[c]	12.0 ± 6.4[c]

[a] Neonatal rat pups were orally infected with 5.0×10^7 wild-type *E. coli* K1 or *traJ* mutant JLB9 bacteria. On day 1 post-oral inoculation, livers and spleens were removed and subjected to immunohistochemistry as described in Materials and Methods. Results are presented as follows: Percent intracellular = (number of stained intracellular bacteria/total number of bacteria associated with positively stained cell) × 100. Data for entire tissue sections (containing 500 to 1,000 positively stained phagocytes and 0 to 500 stained *E. coli* K1 bacteria) from several experiments were averaged and are presented as means ± SEM. tMO, tissue macrophage; DC, dendritic cell.

[b] Significantly different from results from the wild type at a P of < 0.004.

[c] Significantly different from results for the wild type at a P of < 0.0001.

does not influence the ability of *E. coli* K1 to survive PMN killing or for PMNs to move chemotactically towards *E. coli* K1 in vitro. Although these data indicate TraJ does not influence PMN chemotaxis to *E. coli* K1 in vitro, it does not rule out the possibility that there may be alterations in chemokine production or activity in wild-type- versus mutant-infected tissues, as has been shown for several other pathogenic bacteria (45). The decrease in virulence of the *traJ* mutant compared to that of the wild type is due, in part, to the ability of the host to recognize, mount an inflammatory response to, and/or effectively kill the infecting mutant bacteria during the oral infection process.

Interestingly, our results elucidate that the mechanism by which TraJ contributes to the early systemic dissemination of *E. coli* K1 in the oral infection process is via specific TraJ-dependent bacterial interactions with macrophages. For example, in vitro, the *traJ* mutant is internalized by macrophages less frequently than wild-type *E. coli* K1. More importantly, we show that post-oral infection in the neonatal rat, TraJ contributes to the ability of *E. coli* K1 to reside within liver and spleen tissue macrophages and dendritic cells and that this association is exclusive to the early dissemination phase of the disease. Furthermore, electron microscopy analysis revealed that there is a distinct difference in the macrophage morphological characteristics of the wild-type and the *traJ* mutant bacteria. Wild-type bacteria were found predominantly within large and spacious phagosomes, whereas the *traJ* mutant bacteria were found to occur intracellularly at a much lower frequency, and when observed, the mutant bacteria were contained within small, tight phagosomal compartments. These distinct morphological processes for the two different strains are reminiscent of two different biological phenomena. For example, recent work by Watarai et al. demonstrated that the type IV secretion system of *Legionella pneumophila*, the Dot/Icm machinery, is necessary for macropinocytic uptake into mouse macrophages (43). Analogous to our study, these investigators noted that wild-type *L. pneumophila* was consistently observed in large concentric vacuoles similar in morphology to fluid-filled macropinosomes. In contrast, the *dotA* mutant bacteria were found in significantly smaller compartments within the

macrophages (43). Our results showing *E. coli* K1 bacteria are in a TraJ-dependent and morphologically distinct intracellular compartment are also reminiscent of the difference between Fc receptor- and complement receptor-mediated phagocytosis. Early electron microscopy studies have shown that particles taken up by macrophages via Fc-receptor-mediated phagocytosis are contained with a spacious phagosome. Conversely, complement receptor-mediated phagocytosis results in the particle contained within small and tight phagosomes (1, 3). Of interest, Fc receptor-mediated phagocytosis is tightly coupled to the production and secretion of proinflammatory molecules (41). In contrast, complement receptor-mediated phagocytosis does not elicit the release of inflammatory mediators. It will be interesting to further investigate the potential relationship between the TraJ-dependent bacterial interactions of macrophages and the potential mechanisms of host inflammatory response in *E. coli* K1 neonatal systemic disease.

Our data indicate that in vitro and in the neonatal rat model of oral infection, macrophages internalize JLB9(*traJ*) at a lower frequency than that of the wild type. In contrast, we found no difference in the abilities of the two strains to invade or survive within epithelial cell lines HEP-2 (human tracheal) or HepG-2 (human liver) or freshly isolated human PMNs or to survive serum killing (unpublished data). Most interestingly, we found that *E. coli* K1 strongly associates in a predominately intracellular nature with respect to lymphoid tissue macrophages and dendritic cells and that this relationship is exclusive to the early stages of systemic dissemination in the neonatal rat. These data are intriguing in that *E. coli* K1 is classically thought to be an antiphagocytic organism. Our data do not contradict this premise but perhaps raise the possibility that the antiphagocytic phenotype is differentially regulated during systemic dissemination. It should be noted that the previous studies elucidating the antiphagocytic phenotype of *E. coli* K1 and its role in pathogenesis have been limited to in vitro systems, examining PMNs, or excluding the early stages of dissemination (10, 11, 12, 16, 28, 37).

One can envision two possible scenarios for the contribution of TraJ to the early dissemination *E. coli* K1 from the MLN to deeper tissues. (i) In the lymphoid tissues, where bacterial clearance principally occurs, the *traJ* mutant is taken up less by professional phagocytes (i.e., tissue macrophages and dendritic cells) than the wild type is, therefore resulting in more extracellular bacteria. As a result, these primarily extracellular bacteria are not in a protective intracellular niche; thus, there are more bacteria for the neutrophils to "see" and mount a host response against (i.e., kill). In this scenario, it may be the case that in these early steps of dissemination, the intracellular environment of the phagocytes provides a protective or safe site from the initial host inflammatory defense mechanisms. In addition, this initial intracellular phase for wild-type *E. coli* K1 may create a sufficient lag time for the bacteria to adequately increase in numbers so as to overcome and/or inhibit the host defenses. (ii) Alternatively, but not exclusively, specific TraJ-dependent interactions between wild-type *E. coli* K1 and macrophages may elicit a modulated cytokine response that results in a more favorable environment for the intra- and/or extracellular bacteria (i.e., altering the inflammatory cytokine network and/or neutrophil chemokine response). Because a *traJ* mutation decreases the ability of the organism to efficiently be taken up by macrophages, yet does not completely abolish internalization by macrophages, and because our TEM analysis demonstrated that there was a distinctive difference between phagosomes containing the wild type (spacious) and those containing the *traJ* mutant (small and tight), there is presumably also a TraJ-independent *E. coli* K1 uptake mechanism. Thus, it is tempting to speculate that because the uptake mechanisms may be different for the two strains, the potential downstream macrophage-elicited inflammatory responses may be dissimilar (i.e., the wild type suppresses inflammatory response or modulates the inflammatory cytokine network via TraJ-dependent interaction with macrophages). Experiments are currently in progress within our laboratory in order to elucidate these and other unknowns in the pathogenesis of neonatal *E. coli* K1 dissemination and systemic infection. Improved knowledge will potentially lead to the development of novel treatments and preventive strategies for this devastating neonatal disease.

ACKNOWLEDGMENTS

We are grateful for George McNamara's expertise and generous assistance in the fluorescent microscopy experiments performed at the CHLA Research Institute Image Core Facility. We thank Earl Leonard for assistance in statistical analysis. We also thank Martine Torres and Robert Weihing for helpful neutrophil biology discussions and technical assistance, respectively. HepG-2 cells were kindly provided by the USC Research Center for Liver Diseases.

This work was funded in part by Public Health Service grant RO1A150675 from NIAID, the CHLA Research Institute Career Development Award, and CHLA Department of Pathology Start-Up Funds to J.L.B.

REFERENCES

1. **Aderem, A., and D. M. Underhill.** 1999. Mechanisms of phagocytosis in macrophages. Annu. Rev. Immunol. **17:**593–623.
2. **Aguero, M. E., G. de la Fuente, E. Vivaldi, and F. Cabello.** 1989. ColV increases the virulence of *Escherichia coli* K1 strains in animal models of neonatal meningitis and urinary infection. Med. Microbiol. Immunol. **178:** 211–216.
3. **Allen, L. A.** 2001. The role of the neutrophil and phagocytosis in infection caused by *Helicobacter pylori*. Curr. Opin. Infect. Dis. **14:**273–277.
4. **Badger, J. L., and K. S. Kim.** 1998. Environmental growth conditions influence the ability of *Escherichia coli* K1 to invade brain microvascular endothelial cells and confer serum resistance. Infect. Immun. **66:**5692–5697.
5. **Badger, J. L., C. A. Wass, and K. S. Kim.** 2000. Identification of *Escherichia coli* K1 genes contributing to human brain microvascular endothelial cell invasion by differential fluorescence induction. Mol. Microbiol. **36**(1)**:**174–182.
6. **Badger, J. L., C. A. Wass, S. J. Weissman, and K. S. Kim.** 2000. Application of signature-tagged mutagenesis for identification of *Escherichia coli* K1 genes that contribute to invasion of human brain microvascular endothelial cells. Infect. Immun. **68:**5056–5061.
7. **Bloch, C. A., and P. E. Orndorff.** 1990. Impaired colonization by and full invasiveness of *Escherichia coli* K1 bearing a site-directed mutation in the type 1 pilin gene. Infect. Immun. **58:**275–278.
8. **Bloch, C. A., B. A. Stocker, and P. E. Orndorff.** 1992. A key role for type 1 pili in enterobacterial communicability. Mol. Microbiol. **6:**697–701.
9. **Bloch, C. A., G. M. Thorne, and F. M. Ausubel.** 1989. General method for site-directed mutagenesis in *Escherichia coli* O18ac:K1:H7: deletion of the inducible superoxide dismutase gene, *sodA*, does not diminish bacteremia in neonatal rats. Infect. Immun. **57:**2141–2148.
10. **Bortolussi, R., P. Ferrieri, B. Björkstén, and P. G. Quie.** 1979. Capsular K1 polysaccharide of *Escherichia coli*: relationship to virulence in newborn rats and resistance to phagocytosis. Infect. Immun. **25:**293–298.
11. **Bortolussi, R., P. Ferrieri, and L. W. Wannamaker.** 1978. Dynamics of *Escherichia coli* infection and meningitis in infant rats. Infect. Immun. **22:** 480–485.
12. **Cross, A. S., K. S. Kim, D. C. Wright, J. C. Sadoff, and P. Gemski.** 1986. Role of lipopolysaccharide and capsule in the serum resistance of bacteremic strains of *Escherichia coli*. J. Infect. Dis. **154:**497–503.

13. **Denholm, E. M., and G. P. Stankus.** 1995. Differential effects of two fluorescent probes on macrophage migration as assessed by manual and automated methods. Cytometry **19:**366–369.
14. **Feigin, R. D.** 1977. Bacterial meningitis in the newborn infant. Clin. Perinatol. **4:**103–116.
15. **Frost, L. S., K. Ippen-Ihler, and R. A. Skurray.** 1994. Analysis of the sequence and gene products of the transfer region of the F sex factor. Microbiol. Rev. **58:**162–210.
16. **Glode, M. P., A. Sutton, E. R. Moxon, and J. B. Robbins.** 1977. Pathogenesis of neonatal *Escherichia coli* meningitis: induction of bacteremia and meningitis in infant rats fed *E. coli* K1. Infect. Immun. **16:**75–80.
17. **Gonzalez, M. D., C. A. Lichtensteiger, and E. R. Vimr.** 2001. Adaptation of signature-tagged mutagenesis to *Escherichia coli* K1 and the infant-rat model of invasive disease. FEMS Microbiol. Lett. **198:**125–128.
18. **Guerina, N. G., T. W. Kessler, V. J. Guerina, M. R. Neutra, H. W. Clegg, S. Langermann, F. A. Scannapieco, and D. A. Goldmann.** 1983. The role of pili and capsule in the pathogenesis of neonatal infection with *Escherichia co*li K1. J. Infect. Dis. **148:**395–405.
19. **Hoffman, J. A., C. Wass, M. F. Stins, and K. S. Kim.** 1999. The capsule supports survival but not traversal of *Escherichia coli* K1 across the blood-brain barrier. Infect. Immun. **67:**3566–3570.
20. **Huang, S.-H., C. Wass, Q. Fu, N. V. Prasadarao, M. Stins, and K. S. Kim.** 1995. *Escherichia coli* invasion of brain microvascular endothelial cells in vitro and in vivo: molecular cloning and characterization of invasion gene ibe10. Infect. Immun. **63:**4470–4475.
21. **Kasper, D. L., J. L. Winkelhake, W. D. Zollinger, B. L. Brandt, and M. S. Artenstein.** 1973. Immunochemical similarity between polysaccharide antigens of *Escherichia coli* 07: K1(L):NM and group B *Neisseria meningitidis*. J. Immunol. **110:**262–268.
22. **Kim, K. S., H. Itabashi, P. Gemski, J. Sadoff, R. L. Warren, and A. S. Cross.** 1992. The K1 capsule is the critical determinant in the development of *Escherichia coli* meningitis in the rat. J. Clin. Investig. **90:**897–905.
23. **Lepay, D. A., C. F. Nathan, R. M. Steinman, H. W. Murray, and Z. A. Cohn.** 1985. Murine Kupffer cells. Mononuclear phagocytes deficient in the generation of reactive oxygen intermediates. J. Exp. Med. **161:**1079–1096.
24. **Leying, H., S. Suerbaum, H.-P. Kroll, D. Stahl, and W. Opferkuch.** 1990. The capsular polysaccharide is a major determinant of serum resistance in K-1-positive blood culture isolates of *Escherichia coli*. Infect. Immun. **58:**222–227.
25. **Martindale, J., D. Stroud, E. R. Moxon, and C. M. Tang.** 2000. Genetic analysis of *Escherichia coli* K1 gastrointestinal colonization. Mol. Microbiol. **37:**1293–1305.
26. **McCracken, G. H., Jr., L. D. Sarff, M. P. Glode, S. G. Mize, M. S. Schiffer, J. B. Robbins, E. C. Gotschlich, I. Orskov, and F. Orskov.** 1974. Relation between *Escherichia coli* K1 capsular polysaccharide antigen and clinical outcome in neonatal meningitis. Lancet **ii:**246–250.
27. **Moxon, E. R., M. P. Glode, A. Sutton, and J. B. Robbins.** 1977. The infant rat as a model of bacterial meningitis. J. Infect. Dis. **136**(Suppl.)**:**S186–S190.
28. **Pluschke, G., J. Mayden, M. Achtman, and R. P. Levine.** 1983. Role of the capsule and the O antigen in resistance of O18:K1 *Escherichia coli* to complement-mediated killing. Infect. Immun. **42:**907–913.
29. **Pluschke, G., A. Mercer, B. Kuseæek, A. Pohl, and M. Achtman.** 1983. Induction of bacteremia in newborn rats by *Escherichia coli* K1 is correlated with only certain O (lipopolysaccharide) antigen types. Infect. Immun. **39:** 599–608.
30. **Prasadarao, N. V., C. A. Wass, J. N. Weiser, M. F. Stins, S.-H. Huang, and K. S. Kim.** 1996. Outer membrane protein A of *Escherichia coli* contributes to invasion of brain microvascular endothelial cells. Infect. Immun. **64:**146–153.
31. **Reed, M. J., and H. Muench.** 1938. A simple method of estimating fifty percent endpoints. Am. J. Hyg. **27:**493–497.
32. **Robbins, J. B., G. H. McCracken, Jr., E. C. Gotschlich, F. Orskov, I. Orskov, and L. A. Hanson.** 1974. *Escherichia coli* K1 capsular polysaccharide associated with neonatal meningitis. N. Engl. J. Med. **290:**1216–1220.
33. **Sarff, L. D., G. H. McCracken, M. S. Schiffer, M. P. Glode, J. B. Robbins, I. Orskov, and F. Orskov.** 1975. Epidemiology of *Escherichia coli* K1 in healthy and diseased newborns. Lancet **i:**1099–1104.
34. **Scannapieco, F. A., N. G. Guerina, and D. A. Goldmann.** 1982. Comparison of virulence and colonizing capacity of *Escherichia coli* K1 and non-K1 strains in neonatal rats. Infect. Immun. **37:**830–832.
35. **Siegel, J. D., and G. H. McCracken, Jr.** 1981. Sepsis neonatorum. N. Engl. J. Med. **304:**642–647.
36. **Smith, H. W., and M. B. Huggins.** 1980. The association of the O18, K1 and H7 antigens and the Co1V plasmid of a strain of *Escherichia coli* with its virulence and immunogenicity. J. Gen. Microbiol. **121:**387–400.
37. **Stevens, P., S. N. Huang, W. D. Welch, and L. S. Young.** 1978. Restricted complement activation by *Escherichia coli* with the K-1 capsular serotype: a possible role in pathogenicity. J. Immunol. **121:**2174–2180.
38. **Taylor, P. W., and H. P. Kroll.** 1983. Killing of an encapsulated strain of *Escherichia coli* by human serum. Infect. Immun. **39:**122–131.
39. **Tunkel, A. R., and W. M. Scheld.** 1993. Pathogenesis and pathophysiology of bacterial meningitis. Clin. Microbiol. Rev. **6:**118–136.
40. **Tunkel, A. R., B. Wispelwey, and W. M. Scheld.** 1990. Pathogenesis and pathophysiology of meningitis. Infect. Dis. Clin. North Am. **4:**555–581.
41. **Underhill, D. M., and A. Ozinsky.** 2002. Phagocytosis of microbes: complexity in action. Annu. Rev. Immunol. **20:**825–852.
42. **van Biesen, T., F. Soderbom, E. G. Wagner, and L. S. Frost.** 1993. Structural and functional analyses of the FinP antisense RNA regulatory system of the F conjugative plasmid. Mol. Microbiol. **10:**35–43.
43. **Watarai, M., I. Derre, J. Kirby, J. D. Growney, W. F. Dietrich, and R. R. Isberg.** 2001. *Legionella pneumophila* is internalized by a macropinocytotic uptake pathway controlled by the Dot/Icm system and the mouse Lgn1 locus. J. Exp. Med. **194:**1081–1096.
44. **Weiser, J. N., and E. C. Gotschlich.** 1991. Outer membrane protein A (OmpA) contributes to serum resistance and pathogenicity of *Escherichia coli* K-1. Infect. Immun. **59:**2252–2258.
45. **Wilson, M., R. Seymour, and B. Henderson.** 1998. Bacterial perturbation of cytokine networks. Infect. Immun. **66:**2401–2409.

Editor: B. B. Finlay